ADVANCED ENERGY MATERIALS

Supporting Information

for *Adv. Energy Mater.,* DOI: 10.1002/aenm.201800087

Sodium-Doped Tin Sulfide Single Crystal: A Nontoxic Earth-Abundant Material with High Thermoelectric Performance

Hong Wu, Xu Lu, Guoyu Wang, Kunling Peng, Hang Chi, Bin Zhang, Yongjin Chen, Chengjun Li, Yanci Yan, Lijie Guo, Ctirad Uher, Xiaoyuan Zhou, and Xiaodong Han**

Supporting information

Sodium-Doped Tin Sulfide Single Crystal: A Nontoxic Earth-Abundant Material with High Thermoelectric Performance

Hong Wu, Xu Lu, Guoyu Wang, Kunling Peng, Hang Chi, Bin Zhang, Yongjin Chen, Chengjun Li, Yanci Yan, Lijie Guo, Ctirad Uher, Xiaoyuan Zhou, Xiaodong Han**

H. Wu, K. L. Peng, C. J. Li, L. J. Guo, Y. C. Yan, Prof. X. Lu, Prof. X.Y Zhou
College of Physics, Chongqing University, Chongqing 401331, P. R. China
Email: xiaoyuan2013@cqu.edu.cn
Y. J. Chen, Prof. X.D. Han
Beijing Key Laboratory of Microstructure and Property of Advanced Materials, Beijing University of Technology, Beijing 100024, P. R. China
Email: xdhan@bjut.edu.cn
Dr. B. Zhang, Prof. X.Y. Zhou
Analytical and Testing Center of Chongqing University, Chongqing 401331, P. R. China
Dr. H. Chi, Prof. C. Uher
Department of Physics, University of Michigan, Ann Arbor, MI48109, USA
H. Wu, Prof. G. Y. Wang
Chongqing Institute of Green and Intelligent Technology, Chinese Academy of Sciences Chongqing 400714, P. R. China and University of Chinese Academy of Sciences, Beijing, 100044, P. R. China

The band effective mass calculations

Figure 3 shows the DFT band structure of SnS in the Pnma phase. Table 1 provides the information (position, effective mass, degeneracy) for the top of the valence band of the SnS crystal. The inertial effective mass tensor is defined as follows:

$$\frac{1}{m_{ij}^{*}} = \frac{1}{\hbar^2}\frac{\partial^2 E_n(\vec{k})}{\partial k_i k_j}, i,j = x,y,z \qquad (S1)$$

where x,y,z are the direction in the reciprocal Cartesian space $(2\pi/A)$; $E_n(\vec{k})$ is the dispersion relation for the *n*-th electronic band; $\hbar$ is the reduced Planck constant; and m_{xx}^{*}, m_{yy}^{*}, and m_{zz}^{*} are the inertial effective masses along the different principal axes of the constant energy ellipsoids. In our case with strong anisotropy, it is necessary to average the

effective masses along different axes. The transport effective mass is calculated by a harmonic mean:

$$m_c^* = 3\left[\frac{1}{m_{xx}^*} + \frac{1}{m_{yy}^*} + \frac{1}{m_{zz}^*}\right]^{-1} \quad \text{(S2)}$$

In general, the transport effective mass is the average inertial effective mass (m_I^*). The total DOS effective mass is defined as follows:

$$m_d^* = N_v{}^{2/3} m_b^* \quad \text{(S3)}$$

with the band effective mass: $m_b^* = \sqrt[3]{m_{xx}^* m_{yy}^* m_{zz}^*}$.

Single band model

In general, when considering transport properties of thermoelectric materials, the band model assumes rigid bands, that is, the electronic structure does not change with respect to light doping and small fluctuations in temperature. Consequently, we investigated the Seebeck coefficients as a function of the carrier density using the parabolic band model. The transport coefficients within a single band approximation can be expressed as follows:

$$S = \pm\frac{k_B}{e}\left(\frac{\left(r+\frac{5}{2}\right)F_{r+\frac{3}{2}}(\eta)}{\left(r+\frac{3}{2}\right)F_{r+\frac{1}{2}}(\eta)} - \eta\right) \quad \text{(S4)}$$

$$r_H = \frac{3}{4}\left(\frac{F_{\frac{1}{2}}(\eta) * F_{-\frac{1}{2}}(\eta)}{F_0(\eta)^2}\right) \quad \text{(S5)}$$

$$n = \frac{(2m^* k_B T)^{3/2} * F_{\frac{1}{2}}(\eta)}{2\pi^2 \hbar^3 r_H} \quad \text{(S6)}$$

$$F_n(\eta) = \int_0^\infty \frac{\chi^n}{1+e^{\chi-\eta}} d\chi \quad \text{(S7)}$$

where η is the reduced Fermi energy, r is the scattering factor, $\hbar$ is the Planck's constant, kB is the Boltzmann constant, e is the electron charge, and m* is the DOS effective mass.

Calculations of the average *zT*

The average (zT_{ave}) is calculated as follows:

$$zT_{ave} = \frac{\int_{T_c}^{T_h} zT(T)\,dT}{T_h - T_c};\ zT(T) = \sum_{i=0}^{5} C_i T^i \qquad (S8)$$

where T_c and T_h are the minimum and maximum temperature, respectively, T is the absolute temperature, and C_i is the fitting constant for each term of T_i.

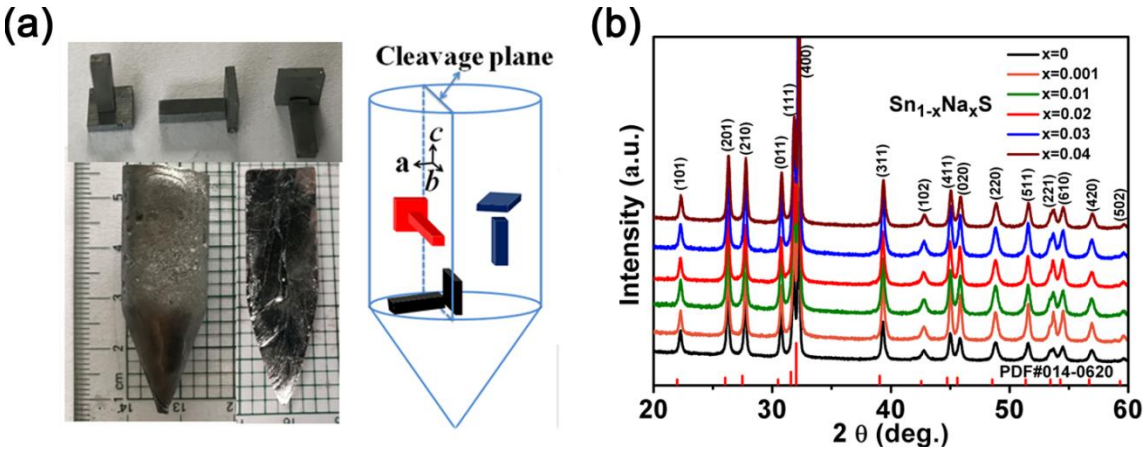

Figure S1. (a) The photos of as-prepared single crystals, cleaved samples, and square-shape samples for measurements of TE properties. (b) XRD diffraction patterns for $Na_xSn_{1-x}S$ powder (x = 0, 0.001, 0.01, 0.02, 0.03, and 0.04).

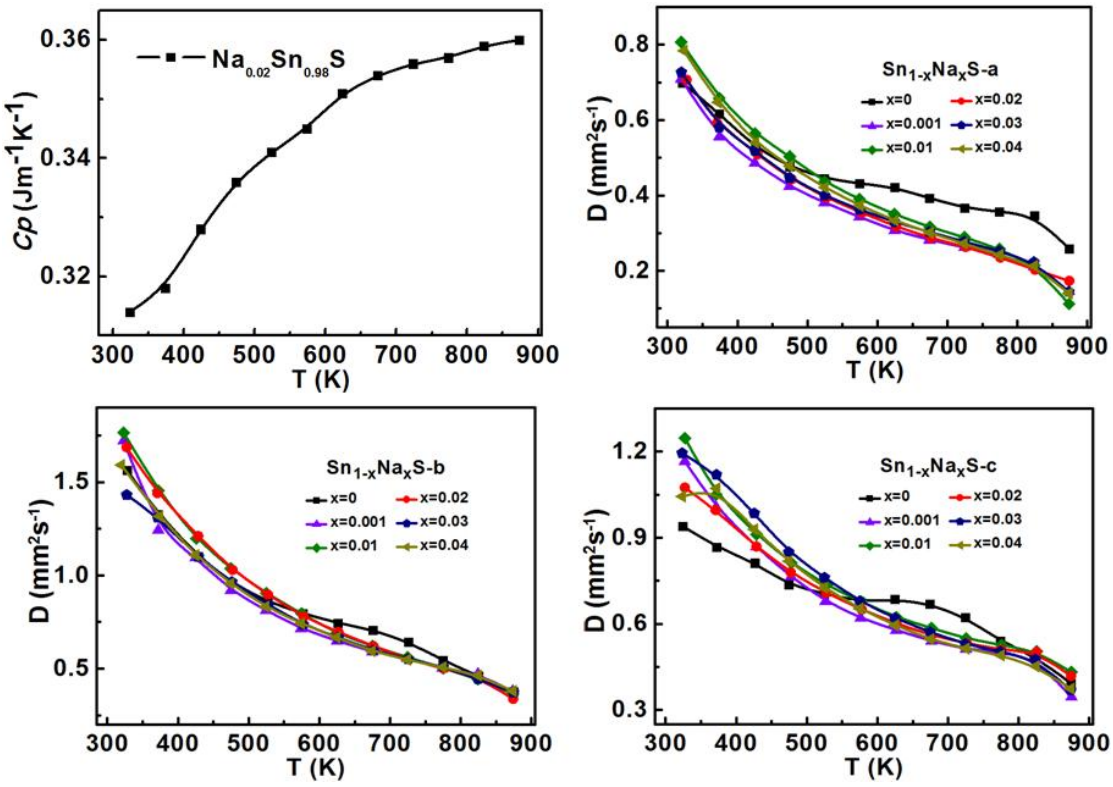

Figure S2. (a) Heat capacity of the $Na_{0.02}Sn_{0.98}S$ single crystal; (b), (c), and (d) thermal diffusion coefficient of all samples along the crystalline *a*-, *b*-, and *c*-axis, respectively.

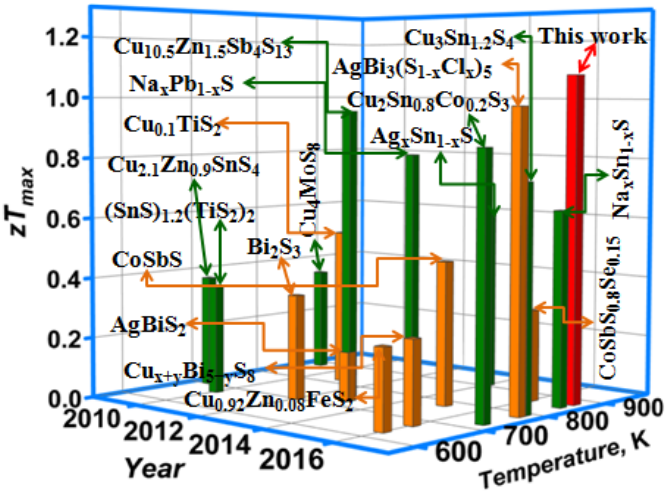

Figure S3. The highest *zT* value of our $Sn_{0.98}Na_{0.02}S$ single crystal (red bar) along with *zT* values for other metal sulfides except for superionic conductors; green and orange bars representing *p*-type and *n*-type materials in the previous literatures,[1-14] respectively.

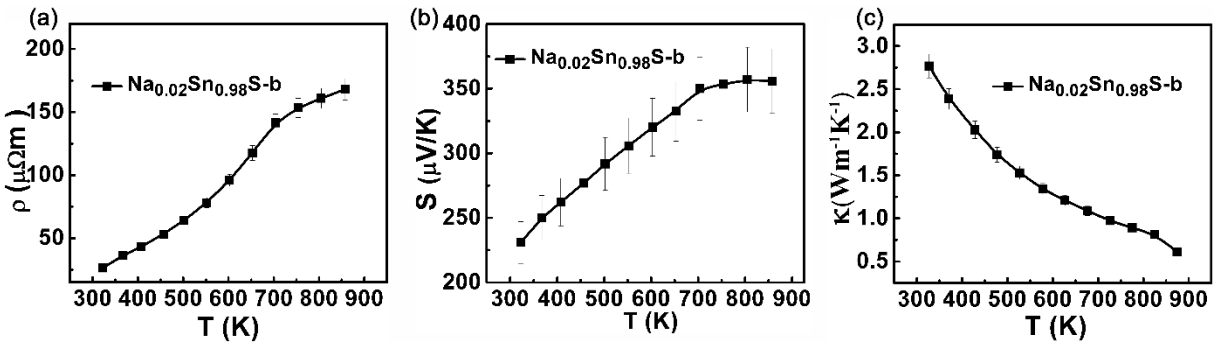

Figure S4. The uncertainties of the thermoelectric properties for $Na_{0.02}Sn_{0.98}S$ single crystal along the *b*-axis: (a) electrical resistivity; (b) Seebeck coefficient; and (c) the total thermal conductivity.

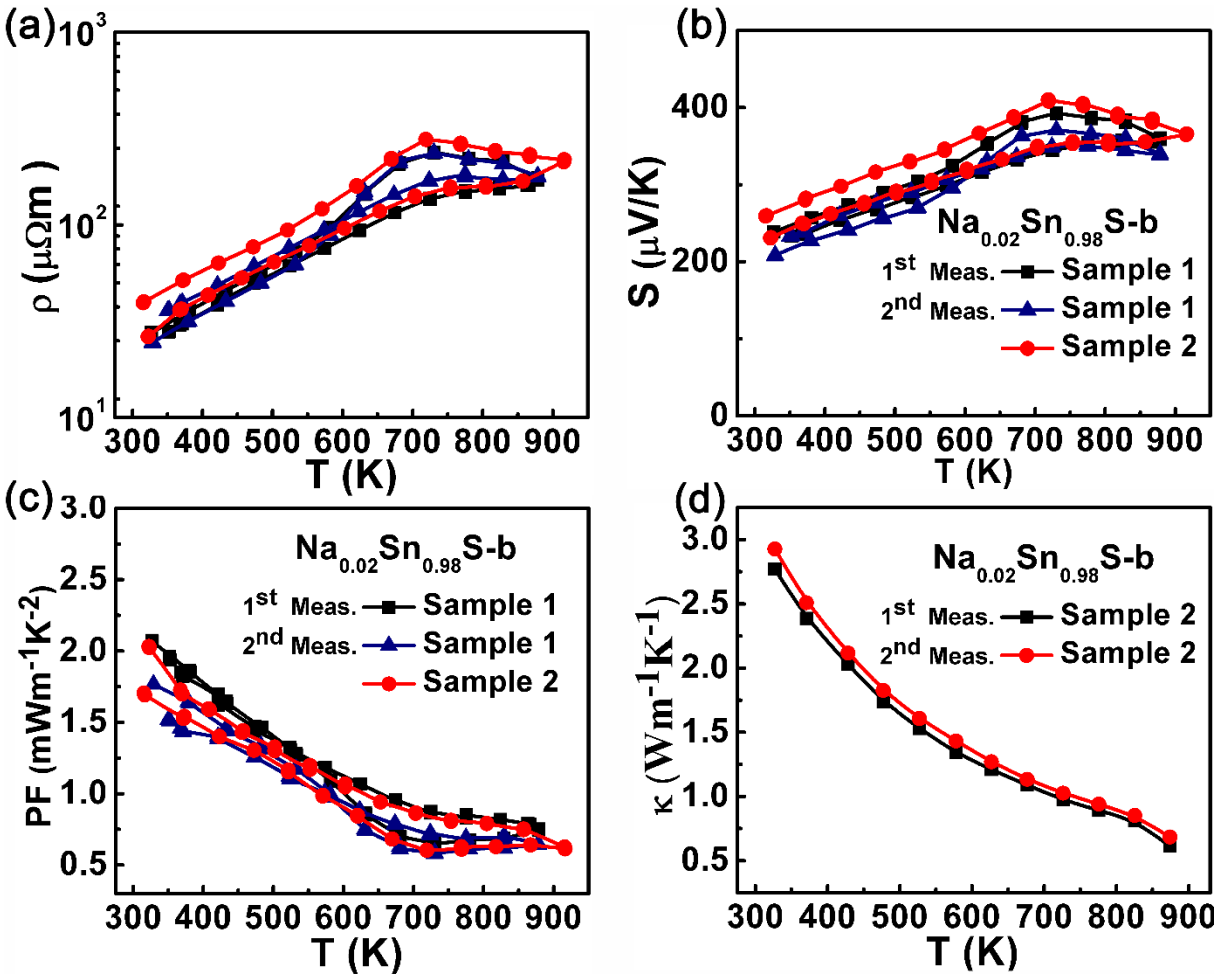

Figure S5. The reproducibility and thermal cycling stability for two $Sn_{0.98}Na_{0.02}S$ single crystal samples along the *b*-axis: (a) electrical resistivity; (b) Seebeck coefficient; (c) power factor; and (d) total thermal conductivity.

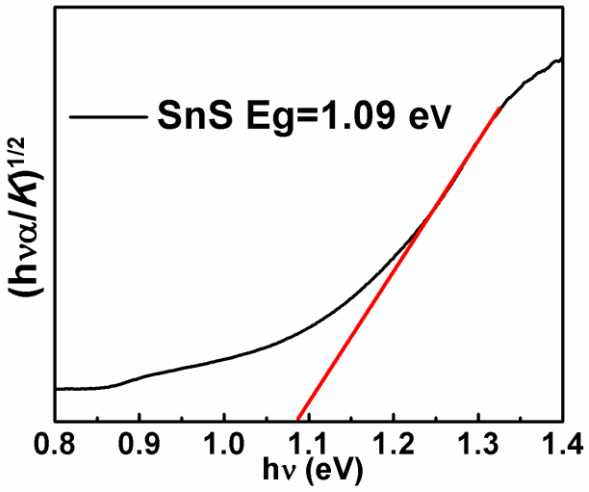

Figure S6. The optical band gap for pristine SnS sample.

Table S1. The sample density and the Rietveld refinement for SnS-*x*%Na (*x* = 0, 0.1, 1, 2, 3, and 4). The standard deviation is roughly 0.0003 and 0.02 for lattice parameters and volume, respectively.

x	*a* (Å)	*b* (Å)	*c* (Å)	Volume(Å^3)	Density(g cm^{-3})
0	11.1914	3.9835	4.3275	192.9216	5.03
0.1	11.1901	3.9831	4.3270	192.8573	5.11
1	11.1916	3.9841	4.3287	193.0062	5.08
2	11.1985	3.9850	4.3297	193.2198	5.12
3	11.1937	3.9848	4.3286	193.0618	5.15
4	11.1952	3.9827	4.3268	192.9198	5.14

Thermoelectric properties as a function of temperature for $Na_xSn_{1-x}S$ powder (*x*=0, 0.001, 0.01, 0.02, 0.03 and 0.04)

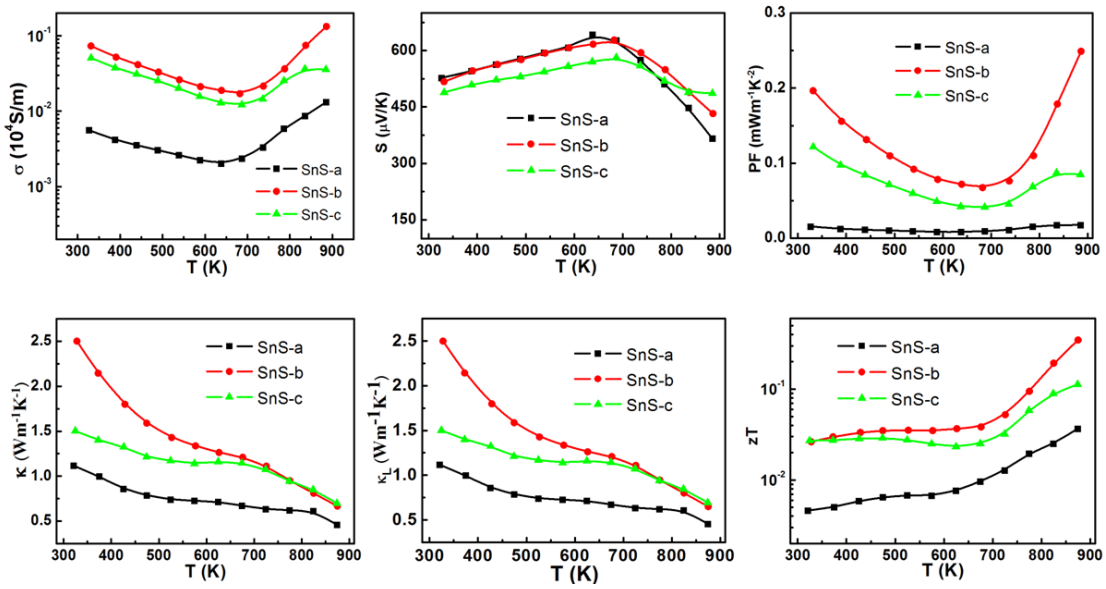

Figure S7. Thermoelectric properties as a function of temperature for SnS.

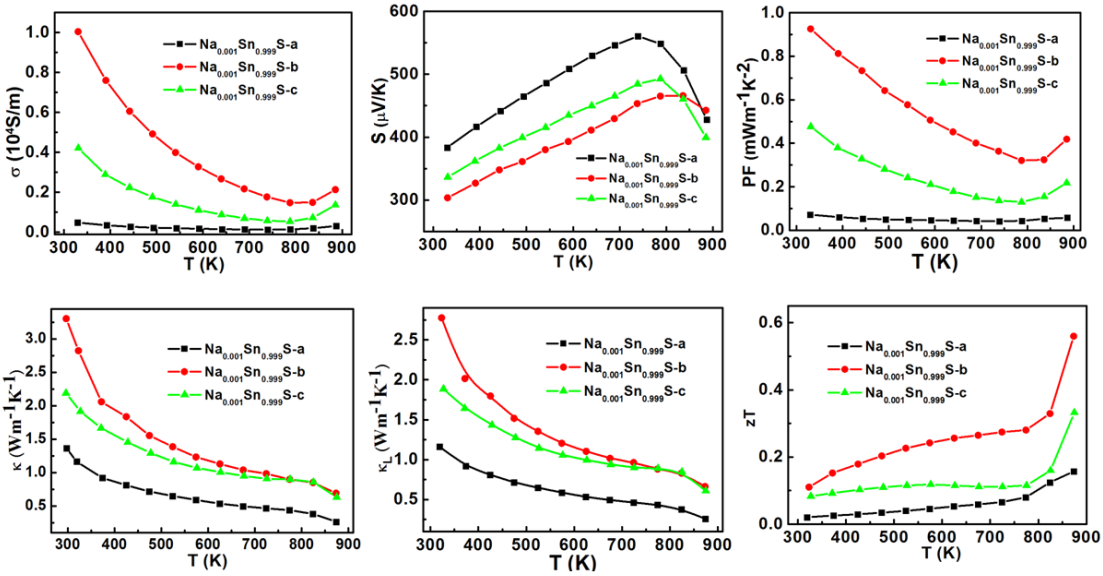

Figure S8. Thermoelectric properties as a function of temperature for $Sn_{0.999}Na_{0.001}S$.

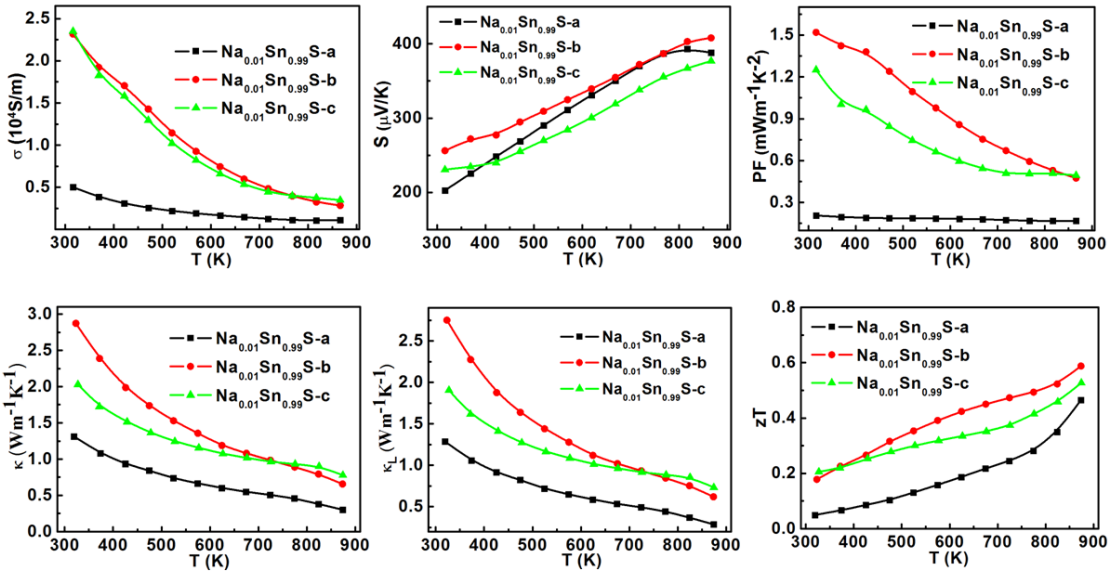

Figure S9. Thermoelectric properties as a function of temperature for $Sn_{0.99}Na_{0.01}S$.

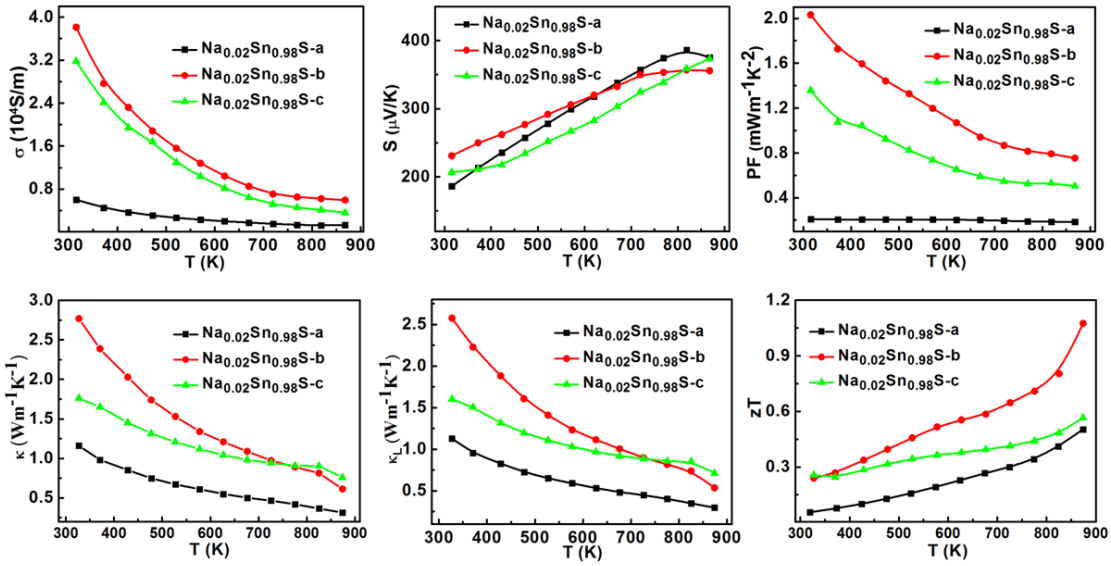

Figure S10. Thermoelectric properties as a function of temperature for $Sn_{0.98}Na_{0.02}S$.

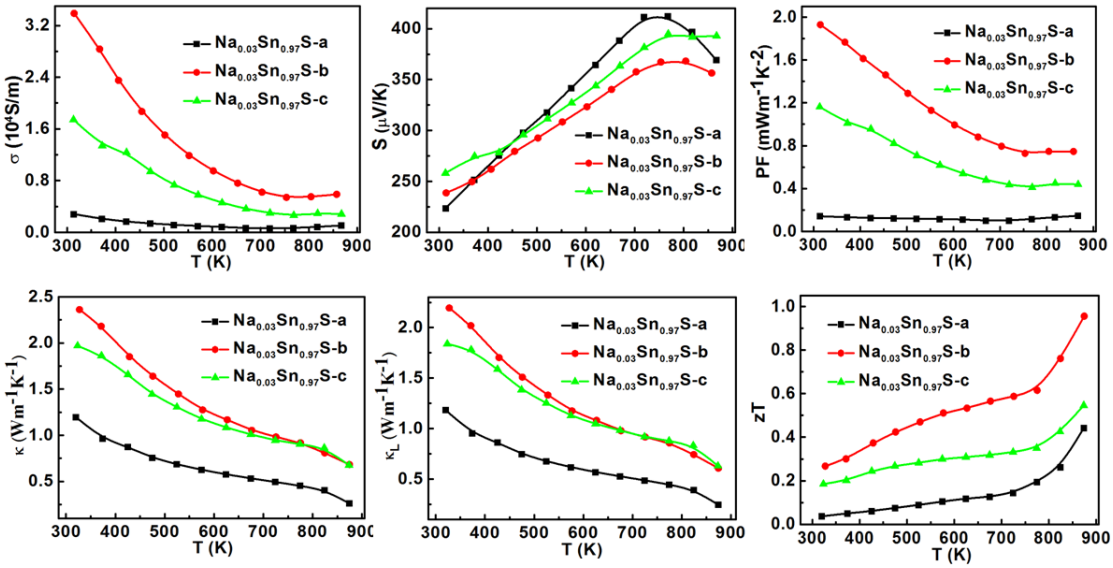

Figure S11. Thermoelectric properties as a function of temperature for $Sn_{0.97}Na_{0.03}S$.

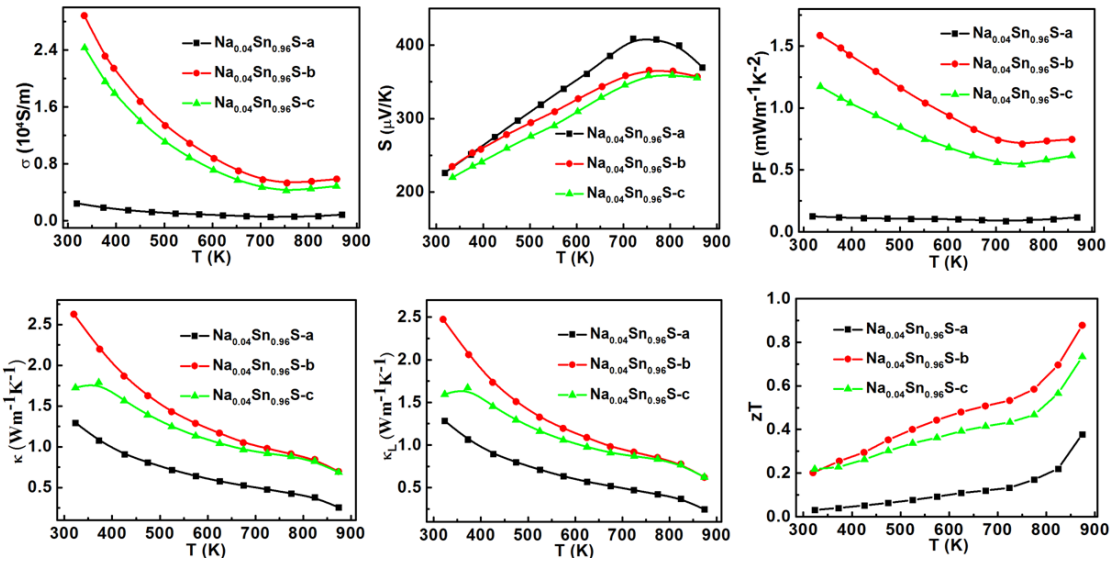

Figure S12. Thermoelectric properties as a function of temperature for $Sn_{0.96}Na_{0.04}S$.

References

[1] W. Yao, D. Yang, Y. Yan, K. Peng, H. Zhan, A. Liu, X. Lu, G. Wang, X. Zhou, *ACS Appl. mater. Interfaces* **2017**, *9*, 10595-10601.

[2] L. D. Zhao, J. He, S. Hao, C. I. Wu, T. P. Hogan, C. Wolverton, V. P. Dravid, M. G. Kanatzidis, *J. Am. Chem. Soc.* **2012**, *134*, 16327-36.

[3] Y. Yang, P. Ying, J. Wang, X. Liu, Z. Du, Y. Chao, J. Cui, *J. Mater. Chem. A* **2017**, *5*, 18808-18815.

[4] H. Xie, X. Su, G. Zheng, T. Zhu, K. Yin, Y. Yan, C. Uher, M. G. Kanatzidis, X. Tang, *Adv. Energy Mater.* **2017**, *7*, 1601299.

[5] C. Wan, Y. Wang, N. Wang, W. Norimatsu, M. Kusunoki, K. Koumoto, *Sci. Technol. Adv. Mater.* **2010**, *11*, 044306.

[6] G. Tan, S. Hao, J. Zhao, C. Wolverton, M. G. Kanatzidis, *J. Am. Chem. Soc.* **2017**, *139*, 6467-6473.

[7] X. Lu, D. T. Morelli, Y. Xia, F. Zhou, V. Ozolins, H. Chi, X. Zhou, C. Uher, *Adv. Energy Mater.* **2013**, *3*, 342-348.

[8] Z. Liu, H. Geng, J. Shuai, Z. Wang, J. Mao, D. Wang, Q. Jie, W. Cai, J. Sui, Z. Ren, *J.*

Mater. Chem. C **2015**, *3*, 10442-10450.

[9] M. L. Liu, F. Q. Huang, L. D. Chen, I. W. Chen, *Appl. Phys. Lett.* **2009**, *94*, 202103.

[10] S. N. Guin, K. Biswas, *Chem. Mater.* **2013**, *25*, 3225-3231.

[11] E. Guilmeau, Y. Bréard, A. Maignan, *Appl. Phys. Lett.* **2011**, *99*, 052107.

[12] K. Biswas, L. D. Zhao, M. G. Kanatzidis, *Adv. Energy Mater.* **2012**, *2*, 634-638.

[13] J. Y. Ahn, J. Y. Hwang, B. K. Ryu, M. W. Oh, K. H. Lee, S. W. Kim, *CrystEngComm.* **2016**, *18*, 1453-1461.

[14] H. W. Zhao, X. X. Xu, C. Li, R. M Tian, R. Z. Zhang, R. Huang, Y. Lu, D. X. Li, X. H. Hu, L. Pan, Y. F. Wang, *J. Mater. Chem. A* **2017**, *5*, 23267-23275